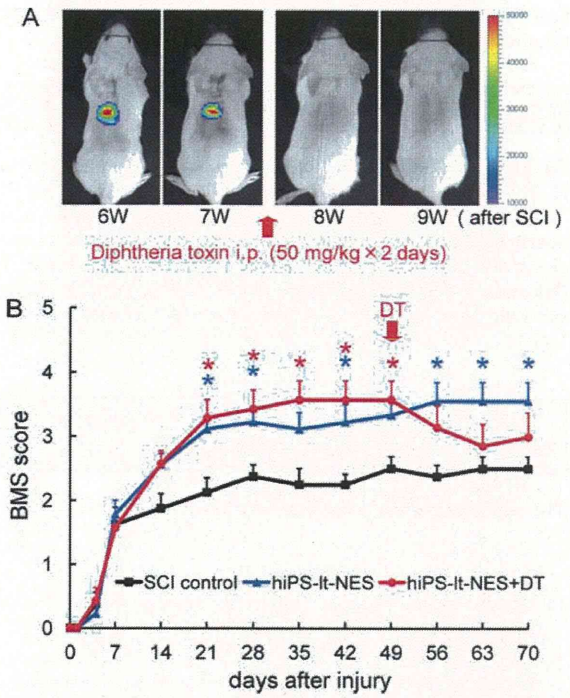

Figure 7. Transplanted cells contribute directly to the functional recovery of hind limb movement in SCI model mice. **(A):** Survival of transplanted cells was monitored using a bioluminescence imaging system. Seven weeks after SCI (6 weeks after transplantation), each mouse was administered DT. One week later, luciferase activity had completely disappeared in hiPS-lt-NES cell-transplanted mice. **(B):** Time course of functional recovery of hind limbs after SCI and DT administration. Data are means ± SEM (SCI control, $n = 8$; hiPS-lt-NES, $n = 9$; and hiPS-lt-NES+DT, $n = 7$). Hind limb function of hiPS-lt-NES cell-transplanted mice deteriorated after DT administration (red line). BMS values of the hiPS-lt-NES and hiPS-lt-NES+DT groups were compared with those of the SCI control group. *, $p < .05$. Abbreviations: BMS, Basso Mouse Scale; DT, diphtheria toxin; hiPS-lt-NES, human induced pluripotent stem cell-derived long-term self-renewing neuroepithelial-like stem; and SCI, spinal cord injury.

C O L O R

further improvements in the treatment of SCI [41]. However, transplantation studies of hiPS-NSCs, initially using mouse models of SCI [9], are in their infancy.

We have previously shown that human lt-NES cells, derived from different hESC and iPSC lines in two independent laboratories, exhibit consistent characteristics and retain their ability to proliferate and differentiate even after several passages and long-term in vitro growth [11]. In the present study, we investigated the differentiation potential of transplanted hiPS-lt-NES cells and found that the majority of differentiated hiPS-lt-NES cells in the injured spinal cord were neurons (Fig. 3D–3F), even though endogenous or transplanted NSCs in the injured spinal cord have been reported by others to differentiate preferentially into the glial lineage [42, 43]. Recent studies have indicated that neurons derived from transplanted human NSCs can integrate into the injured spinal cord and form synaptic connections with host neurons [33, 34]. We therefore took advantage of the tendency of our hiPS-lt-NES cells to differentiate into neurons and tried to apply these cells to reconstruction of the injured spinal cord.

Multiple therapeutic effects of NSC transplantation have been reported, and many different types of stem cells have been grafted into the injured spinal cord, yielding improved functional recovery in animal models [44, 45]. However, the growth of axons through the lesion to reinnervate the side caudal to the injury has so far been very limited. Our experiments using anterograde labeling of CST fibers revealed that this was also the case after transplantation of hiPS-lt-NES cells (Fig. 4). We have previously shown that neurons derived from mouse NSCs could restore disrupted neuronal circuits [15]. Consistent with that observation, we demonstrated here that WGA-positive cell numbers in hiPS-lt-NES cell-treated mice were higher than those in SCI control mice in the area caudal to the SCI (Fig. 5A, 5B). Furthermore, immunohistochemistry using species-specific antibodies for presynaptic markers suggested that transplant-derived neurons made synapses with endogenous neurons (Fig. 5C-2, 5C-2′, 5C-3, and 5C-3′). These results suggest that WGA was transferred to the caudal area through the lesion site via new synaptic connections, and that hiPS-lt-NES cell transplantation promoted CST reconstruction in a relay fashion. Other studies have provided evidence that local neurons can form intraspinal neural circuits in the lesion site and make synaptic connections with descending-tract collaterals after SCI [32, 46], and human NSCs transplanted into the injured rat or mouse spinal cord differentiated into neurons that formed axons and synapses, and also established contacts with host neurons [4, 34].

As well as their roles in cell replacement, NSCs reportedly exert other effects through the secretion of neurotrophic factors [37], which, by means such as suppressing myelin inhibitors, prevent neuronal cell death, enhance remyelination and regenerate axons [47, 48]. We found that transplantation of hiPS-lt-NES cells supported the survival of endogenous neurons (Fig. 6). Conversely, ablation of transplanted cells decreased previously attained functional recovery (Fig. 7), suggesting that transplanted cells contribute directly to functional recovery of hind limb movement in SCI model mice. In summary, we suggest that not only neurons derived from transplanted hiPS-lt-NES cells but also surviving endogenous neurons contribute to functional improvement by forming multiple synaptic connections which restore disrupted neuronal circuits.

Following injury, demyelinated and reconstructed axons must be remyelinated to ensure proper functional recovery. Generally, endogenous or transplanted NSCs which differentiate into oligodendrocytes have been reported to contribute to remyelination of axons and thereby to help in recovery after SCI. Transplanted oligodendrocyte progenitor cells (OPCs) derived from human ESCs have been shown to differentiate into oligodendrocytes and enhance remyelination in the moderate rat model of contusion spinal cord injury [5, 6]. A further study reported that in complete spinal cord transection rats, locomotor recovery after transplantation with both OPCs and human ESC-derived motor neuron progenitor cells was significantly greater than after treatment with either cell type alone [49]. Given that the application of stem cells and their progenitors for transplantation is currently in its infancy, and that SCI pathology differs between contusion and transection [50], these findings indicate that neural cells in an appropriate lineage should be transplanted according to the degree and/or type of SCI.

When ES and iPS cells are used for transplantation treatment, a key consideration is the likelihood of tumor formation, since the transplanted cell population may include undifferentiated cells [51, 52]. Indeed, the sources and methods of induction of NSCs are critical for differentiation and tumor formation [33, 53]. Neurosphere cultures are heterogeneous and sensitive to variations in methodological procedures [12], whereas monolayer cell cultures give rise to more homogeneous population [13, 14]. In this study, we detected no tumor

formation in more than 40 hiPS-lt-NES cell-treated mice up to 12 weeks after SCI. This is probably attributable to complete differentiation of hiPS cells into NES cells in our robust and stable monolayer cell cultures, since the NES cells were established by initially purifying neural rosette structures from differentiating cultures [11]. Furthermore, we transplanted hiPS-lt-NES cells which had been expanded in the presence of growth factors and passaged more than 20 times. Before human iPS cell-based therapies can be implemented for clinical application, the cells' proliferation and tumor formation after transplantation must be strictly evaluated.

In this study, we have demonstrated that hiPS-lt-NES cells survived and differentiated in the injured spinal cord of NOD-SCID mice, and promoted functional recovery of hind limbs. Moreover, we have shown that transplanted hiPS-lt-NES cells support the reconstruction of CST pathways, promote endogenous neuron survival, and directly contribute to improved hind limb movement. To achieve a more efficient treatment for SCI, detailed investigations of hiPS-lt-NES cells and SCI pathology will be necessary. Nevertheless, our study raises the possibility that hiPS-based therapy can be applied in the near future to SCI patients who currently have few or no therapeutic options.

Acknowledgments

We thank M. Saito and K. Kohno for providing diphtheria toxin, H. Miyoshi, H. J. Okano, and H. Okano for lentiviral vectors, Y. Yoshihara for WGA-expressing adenovirus, N. Uchida for anti-human specific antibodies, and S. Nori and M. Nakamura for species-specific antibodies. We also thank Y. Bessho, T. Matsui, Y. Nakahata, T. Matsuda, S. Komai, and M. Arai for valuable discussions and technical advice, T. Matta for statistical analysis, I. Smith for editing the manuscript, and M. Tano for secretarial assistance.

Disclosure of Potential Conflicts of Interest

The authors indicate no potential conflicts of interest.

References

1 Ditunno JF, Formal CS. Chronic spinal cord injury. N Engl J Med 1994;330:550–556.
2 Ogawa Y, Sawamoto K, Miyata T et al. Transplantation of in vitro-expanded fetal neural progenitor cells results in neurogenesis and functional recovery after spinal cord contusion injury in adult rats. J Neurosci Res 2002;69:925–933.
3 Iwanami A, Kaneko S, Nakamura M et al. Transplantation of human neural stem cells for spinal cord injury in primates. J Neurosci Res 2005;80:182–190.
4 Cummings BJ, Uchida N, Tamaki SJ et al. Human neural stem cells differentiate and promote locomotor recovery in spinal cord-injured mice. Proc Natl Acad Sci USA 2005;102:14069–14074.
5 Keirstead HS, Nistor G, Bernal G et al. Human embryonic stem cell-derived oligodendrocyte progenitor cell transplants remyelinate and restore locomotion after spinal cord injury. J Neurosci 2005;25:4694–4705.
6 Sharp J, Frame J, Siegenthaler M et al. Human embryonic stem cell-derived oligodendrocyte progenitor cell transplants improve recovery after cervical spinal cord injury. Stem Cells 2010;28:152–163.
7 Takahashi K, Yamanaka S. Induction of pluripotent stem cells from mouse embryonic and adult fibroblast cultures by defined factors. Cell 2006;126:663–676.
8 Takahashi K, Tanabe K, Ohnuki M et al. Induction of pluripotent stem cells from adult human fibroblasts by defined factors. Cell 2007;131:861–872.
9 Nori S, Okada Y, Yasuda A et al. Grafted human-induced pluripotent stem-cell-derived neurospheres promote motor functional recovery after spinal cord injury in mice. Proc Natl Acad Sci USA 2011.
10 Koch P, Opitz T, Steinbeck JA et al. A rosette-type, self-renewing human ES cell-derived neural stem cell with potential for in vitro instruction and synaptic integration. Proc Natl Acad Sci USA 2009;106:3225–3230.
11 Falk A, Koch P, Kesavan J et al. Capture of neuroepithelial-like stem cells from pluripotent stem cells provides a versatile system for in vitro production of human neurons. PLoS One 2012;7:e29597.
12 Kim HT, Kim IS, Lee IS et al. Human neurospheres derived from the fetal central nervous system are regionally and temporally specified but are not committed. Exp Neurol 2006;199:222–235.
13 Conti L, Pollard SM, Gorba T et al. Niche-independent symmetrical self-renewal of a mammalian tissue stem cell. PLoS Biol 2005;3:e283.
14 Pollard SM, Conti L, Sun Y et al. Adherent neural stem (NS) cells from fetal and adult forebrain. Cereb Cortex 2006;16 Suppl 1:i112–i120.
15 Abematsu M, Tsujimura K, Yamano M et al. Neurons derived from transplanted neural stem cells restore disrupted neuronal circuitry in a mouse model of spinal cord injury. J Clin Invest 2010;120:3255–3266.
16 Sun Y, Pollard S, Conti L et al. Long-term tripotent differentiation capacity of human neural stem (NS) cells in adherent culture. Mol Cell Neurosci 2008;38:245–258.
17 Miyoshi H, Blömer U, Takahashi M et al. Development of a self-inactivating lentivirus vector. J Virol 1998;72:8150–8157.
18 Okada S, Ishii K, Yamane J et al. In vivo imaging of engrafted neural stem cells: Its application in evaluating the optimal timing of transplantation for spinal cord injury. FASEB J 2005;19:1839–1841.
19 Basso DM, Fisher LC, Anderson AJ et al. Basso Mouse Scale for locomotion detects differences in recovery after spinal cord injury in five common mouse strains. J Neurotrauma 2006;23:635–659.
20 Setoguchi T, Nakashima K, Takizawa T et al. Treatment of spinal cord injury by transplantation of fetal neural precursor cells engineered to express BMP inhibitor. Exp Neurol 2004;189:33–44.
21 Hata K, Fujitani M, Yasuda Y et al. RGMa inhibition promotes axonal growth and recovery after spinal cord injury. J Cell Biol 2006;173:47–58.
22 Kaneko S, Iwanami A, Nakamura M et al. A selective Sema3A inhibitor enhances regenerative responses and functional recovery of the injured spinal cord. Nat Med 2006;12:1380–1389.
23 Pronichev IV, Lenkov DN. Functional mapping of the motor cortex of the white mouse by a microstimulation method. Neurosci Behav Physiol 1998;28:80–85.
24 Yoshihara Y, Mizuno T, Nakahira M et al. A genetic approach to visualization of multisynaptic neural pathways using plant lectin transgene. Neuron 1999;22:33–41.
25 Kinoshita N, Mizuno T, Yoshihara Y. Adenovirus-mediated WGA gene delivery for transsynaptic labeling of mouse olfactory pathways. Chem Senses 2002;27:215–223.
26 Furukawa N, Saito M, Hakoshima T et al. A diphtheria toxin receptor deficient in epidermal growth factor-like biological activity. J Biochem 2006;140:831–841.
27 Saito M, Iwawaki T, Taya C et al. Diphtheria toxin receptor-mediated conditional and targeted cell ablation in transgenic mice. Nat Biotechnol 2001;19:746–750.
28 Luchetti S, Beck KD, Galvan MD et al. Comparison of immunopathology and locomotor recovery in C57BL/6, BUB/BnJ, and NOD-SCID mice after contusion spinal cord injury. J Neurotrauma 2010;27:411–421.
29 Yan J, Welsh AM, Bora SH et al. Differentiation and tropic/trophic effects of exogenous neural precursors in the adult spinal cord. J Comp Neurol 2004;480:101–114.
30 Nothias JM, Mitsui T, Shumsky JS et al. Combined effects of neurotrophin secreting transplants, exercise, and serotonergic drug challenge improve function in spinal rats. Neurorehabil Neural Repair 2005;19:296–312.
31 Kim D, Murray M, Simansky KJ. The serotonergic 5-HT(2C) agonist *m*-chlorophenylpiperazine increases weight-supported locomotion without development of tolerance in rats with spinal transections. Exp Neurol 2001;169:496–500.
32 Courtine G, Song B, Roy RR et al. Recovery of supraspinal control of stepping via indirect propriospinal relay connections after spinal cord injury. Nat Med 2008;14:69–74.
33 Hooshmand MJ, Sontag CJ, Uchida N et al. Analysis of host-mediated repair mechanisms after human CNS-stem cell transplantation for spinal cord injury: Correlation of engraftment with recovery. PLoS One 2009;4:e5871.
34 Yan J, Xu L, Welsh AM et al. Extensive neuronal differentiation of human neural stem cell grafts in adult rat spinal cord. PLoS Med 2007;4:e39.

35 Nakamura M, Houghtling RA, MacArthur L et al. Differences in cytokine gene expression profile between acute and secondary injury in adult rat spinal cord. Exp Neurol 2003;184:313–325.
36 Bareyre FM, Schwab ME. Inflammation, degeneration and regeneration in the injured spinal cord: insights from DNA microarrays. Trends Neurosci 2003;26:555–563.
37 Lu P, Tuszynski MH. Growth factors and combinatorial therapies for CNS regeneration. Exp Neurol 2008;209:313–320.
38 Okita K, Nakagawa M, Hyenjong H et al. Generation of mouse induced pluripotent stem cells without viral vectors. Science 2008; 322:949–953.
39 Zhou H, Wu S, Joo JY et al. Generation of induced pluripotent stem cells using recombinant proteins. Cell Stem Cell 2009;4:381–384.
40 Kaji K, Norrby K, Paca A et al. Virus-free induction of pluripotency and subsequent excision of reprogramming factors. Nature 2009;458: 771–775.
41 Lindvall O, Kokaia Z. Stem cells in human neurodegenerative disorders–time for clinical translation? J Clin Invest 2010;120:29–40.
42 Cao QL, Howard RM, Dennison JB et al. Differentiation of engrafted neuronal-restricted precursor cells is inhibited in the traumatically injured spinal cord. Exp Neurol 2002;177:349–359.
43 Han SS, Kang DY, Mujtaba T et al. Grafted lineage-restricted precursors differentiate exclusively into neurons in the adult spinal cord. Exp Neurol 2002;177:360–375.
44 Louro J, Pearse DD. Stem and progenitor cell therapies: recent progress for spinal cord injury repair. Neurol Res 2008;30:5–16.
45 Jain KK. Cell therapy for CNS trauma. Mol Biotechnol 2009;42: 367–376.
46 Bareyre FM, Kerschensteiner M, Raineteau O et al. The injured spinal cord spontaneously forms a new intraspinal circuit in adult rats. Nat Neurosci 2004;7:269–277.
47 Shumsky JS, Tobias CA, Tumolo M et al. Delayed transplantation of fibroblasts genetically modified to secrete BDNF and NT-3 into a spinal cord injury site is associated with limited recovery of function. Exp Neurol 2003;184:114–130.
48 Tobias CA, Shumsky JS, Shibata M et al. Delayed grafting of BDNF and NT-3 producing fibroblasts into the injured spinal cord stimulates sprouting, partially rescues axotomized red nucleus neurons from loss and atrophy, and provides limited regeneration. Exp Neurol 2003;184: 97–113.
49 Erceg S, Ronaghi M, Oria M et al. Transplanted oligodendrocytes and motoneuron progenitors generated from human embryonic stem cells promote locomotor recovery after spinal cord transection. Stem Cells 2010;28:1541–1549.
50 Siegenthaler MM, Tu MK, Keirstead HS. The extent of myelin pathology differs following contusion and transection spinal cord injury. J Neurotrauma 2007;24:1631–1646.
51 Miura K, Okada Y, Aoi T et al. Variation in the safety of induced pluripotent stem cell lines. Nat Biotechnol 2009;27:743–745.
52 Tsuji O, Miura K, Okada Y et al. Therapeutic potential of appropriately evaluated safe-induced pluripotent stem cells for spinal cord injury. Proc Natl Acad Sci USA 2010;107:12704–12709.
53 Jensen JB, Parmar M. Strengths and limitations of the neurosphere culture system. Mol Neurobiol 2006;34:153–161.

See www.StemCells.com for supporting information available online.

STEM CELLS®

TISSUE-SPECIFIC STEM CELLS

Oxygen Levels Epigenetically Regulate Fate Switching of Neural Precursor Cells via Hypoxia-Inducible Factor 1α-Notch Signal Interaction in the Developing Brain

TETSUJI MUTOH, TSUKASA SANOSAKA, KEI ITO, KINICHI NAKASHIMA

Laboratory of Molecular Neuroscience, Graduate School of Biological Sciences, Nara Institute of Science and Technology, Ikoma, Nara, Japan

Key Words. Neural precursor cell • Astrocyte differentiation • DNA methylation • Epigenetic gene regulation • Notch signaling • Oxygen concentration

ABSTRACT

Oxygen levels in tissues including the embryonic brain are lower than those in the atmosphere. We reported previously that Notch signal activation induces demethylation of astrocytic genes, conferring astrocyte differentiation ability on midgestational neural precursor cells (mgNPCs). Here, we show that the oxygen sensor hypoxia-inducible factor 1α (HIF1α) plays a critical role in astrocytic gene demethylation in mgNPCs by cooperating with the Notch signaling pathway. Expression of constitutively active HIF1α and a hyperoxic environment, respectively, promoted and impeded astrocyte differentiation in the developing brain. Our findings suggest that hypoxia contributes to the appropriate scheduling of mgNPC fate determination. STEM CELLS *2012;30:561–569*

Disclosure of potential conflicts of interest is found at the end of this article.

INTRODUCTION

The mammalian embryonic brain contains multipotent neural precursor cells (NPCs) that can self-renew and give rise to all three major cell types in the nervous system, that is, neurons, astrocytes, and oligodendrocytes. NPC fate determination is regulated by the collaboration between cell-external cues, from molecules such as cytokines and growth factors, and cell-internal epigenetic programs [1].

We and others have shown that members of the interleukin-6 (IL-6) family of cytokines, including leukemia inhibitory factor (LIF), efficiently induce astrocyte differentiation of late-gestational (lg) NPCs by activating the janus kinase (JAK)-signal transducer and activator of transcription (STAT) signaling pathway [2, 3]. In contrast to lgNPCs, midgestational (mg) NPCs differentiate only into neurons because the promoters of astrocytic genes, such as that encoding the typical astrocytic marker glial fibrillary acidic protein (GFAP), are hypermethylated at this stage [4, 5]. These findings indicate that DNA methylation is a critical determinant for the acquisition of astrocyte differentiation ability by NPCs [6]. Notch receptors and their ligands, molecules best known for influencing cell fate decisions through direct cell-cell contact, participate in a wide variety of biological processes, including fate determination of NPCs. As gestation proceeds, mgNPCs generate committed neuronal precursors (or young neurons) expressing Notch ligands, and these cells activate Notch signaling in neighboring NPCs. Notch signal activation induces the demethylation of astrocytic gene promoters in NPCs, which explains, at least in part, how the neuronal-to-glial cell fate switch occurs in NPCs during brain development [1, 6, 7].

Oxygen is essential for cell survival as the final electron acceptor in the electron transport chain of aerobic respiration. Sensing and controlling oxygen localization are of extreme importance because normal metabolic processes generate radical intermediates. When oxygen levels exceed the capacity of endogenous antioxidant systems, radicals including reactive oxygen species attack cellular components such as nucleic acids, the sulfhydryl groups of proteins, or the unsaturated fatty acid moieties of phospholipids [8].

Hypoxia-inducible factors (HIFs) are known to play critical roles as molecular sensors of oxygen tension. HIF1α activity in cells is controlled by oxygen levels in multiple ways, such as transcriptional regulation and hydroxylation-dependent binding by Von Hippel-Lindau tumor suppressor protein followed by proteasomal degradation [9–11]. A HIF1 complex composed of HIF1α and HIF1β (also known as ARNT) binds to the hypoxia response element and activates the transcription of target genes such as *inhibitor of differentiation 2* [12], *insulin-like growth factor binding protein*, *p21*, *phosphoglycerate kinase 1*, and *vascular endothelial growth factor* [13].

Author contribution: T.M.: conception and design, financial support, administrative support, provision of study material or patients, collection and/or assembly of data, data analysis and interpretation, and manuscript writing; T.S.: administrative support, collection and/or assembly of data, and data analysis and interpretation; K.I.: provision of study material or patients; and K.N.: conception and design, financial support, administrative support, data analysis and interpretation, and final approval of manuscript. T.M. and T.S. contributed equally to this study.

Correspondence: Kinichi Nakashima, Ph.D., Laboratory of Molecular Neuroscience, Graduate School of Biological Sciences, Nara Institute of Science and Technology, Ikoma, Nara 630-0192, Japan. Telephone: 81-743-72-5471; Fax: 81-743-72-5479; e-mail: kin@bs.naist.jp Received July 19, 2011; accepted for publication December 2, 2011; first published online in STEM CELLS *EXPRESS* December 29, 2011. 1066-5099/2011/$30.00/0 doi: 10.1002/stem.1019

HIF1α has also been reported to be crucial for normal brain development [14]. Moreover, HIFs may act cooperatively with other signaling molecules, such as Notch [15] and mammalian target of rapamycin [16, 17], thereby influencing a wide range of processes including tumor malignancy and NPC growth, maintenance and differentiation [11, 18-20].

In this study, we focused on how oxygen tension affects the DNA methylation status of astrocytic genes in mgNPCs. Oxygen levels in the microenvironment around NPCs in the embryonic brain at midgestation were comparable to those seen under hypoxic culture conditions (2-5% O_2). Bisulfite sequencing revealed that these conditions promoted demethylation of the *gfap* promoter. This hypoxia-induced demethylation was mediated by cooperation between HIF1α and the Notch signaling pathway. Furthermore, ectopic expression of a constitutively active form of HIF1α in the embryonic brain induced precocious astrocyte differentiation of NPCs. By contrast, when embryos developed in hyperoxic conditions, astrocyte differentiation of NPCs was suppressed. These findings suggest that oxygen levels in the embryonic brain play a critical role in fine-tuning the timing of NPC fate switching during development.

Materials and Methods

Cell Culture

mgNPCs were prepared from telencephalons of E11.5 embryos and cultured as described previously [5]. E15.5 ventricular zone (VZ) containing NPCs was manually separated from other parts of the brain using a hand-made microknife (Supporting Information Fig. S1). As described previously [5], NPCs were cultured with basic fibroblast growth factor (bFGF; 1×10^6 cells per dish) in poly-L-ornithine/fibronectin-coated 6-cm culture dishes. Hand-made chambers were used to obtain atmospheres of different oxygen levels [21]. Notch signal activation was inhibited with the γ-secretase inhibitor *N*-[*N*-(3,5-difluorophenacetyl-L-alanyl)]-*S*-phenylglycine *t*-butyl ester (DAPT; Calbiochem-MERCK, Darmstadt, Germany, www.merckgroup.com, 10 μM).

Bisulfite Sequencing

Genomic DNA was extracted from NPCs and subjected to bisulfite sequencing as previously described [5]. Specific DNA fragments were amplified by polymerase chain reaction (PCR) using primers described previously [5, 7]. The PCR products were cloned into pT7Blue vector (Novagen, Darmstadt, Germany, www.merckgroup.com/en/index.html), and 10-20 randomly picked clones were sequenced. Each experiment was performed at least tree times.

Lentivirus Production

A mouse *HIF1α*-targeting short hairpin RNA (shRNA) sequence [22] was cloned into pLLX vector [23]. Lentiviruses were pseudotyped with the vesicular somatitis virus–G envelope and concentrated by centrifugation as previously described [24]. *HIF1α* mRNA degradation was confirmed by quantitative PCR (qPCR). All the recombinant DNA experiments in this manuscript followed the guidelines by Ministry of Education, Culture, Sports, Science and Technology of Japan, which conform to the National Institutes of Health Guidelines.

Immunostaining

Cells were fixed with 4% paraformaldehyde and processed for immunostaining as described [5]. The following primary antibodies were used: chick anti-green fluorescent protein (anti-GFP; 1:500, Aves Labs, Tigard, OR, www.aveslab.com), rat anti-hemagglutinating (anti-HA) (1:500, Roche Applied Science, Indianapolis, IN, www.roche-applied-science.com), rat anti-bromodeoxyuridine (1:250, AbD Serotec, Raleigh, NC, www.abdserotec.com) chicken anti-Nestin (1:1000, Aves Labs), mouse anti-Map2ab (1:500, Sigma, St. Louis, MO, www.sigmaaldrich.com), and mouse anti-GFAP (1:500, Sigma). Secondary antibodies were Alexa488-conjugated goat anti-rat IgG (1:500), Alexa488-conjugated goat anti-chick IgY (1:500), Alexa555-conjugated goat anti-rabbit IgG (1:500), Alexa555-conjugated goat anti-rat IgG (1:500), Alexa555-conjugated goat anti-mouse IgG (1:500), or Alexa647-conjugated goat anti-mouse IgG (1:500, Invitrogen, Carlsbad, CA, www.invitrogen.com). Nuclei were stained using bisbenzimide H33258 fluorochrome trihydrochloride (Hoechst; Nacalai Tesque, Kyoto, Japan, www.nacalai.co.jp). All experiments were independently replicated at least three times. A Hypoxyprobe-1 Plus kit (Hypoxyprobe-Millipore, Billerica, MA, www.millipore.com) was used, following the manufacturer's protocol, to determine the hypoxicity of cultured cells and the developing brain. After culturing NPCs for 4 days in 2%, 5%, or 21% O_2, pimonidazole-HCl was added to the culture medium for 1.5 hours and the cells were then fixed. For brain sections, pimonidazole-HCl was injected intraperitoneally into pregnant mice (E15.5). Embryos were fixed 2 hours later with 4% paraformaldehyde and the brains were cryosectioned at 20-μm intervals. Pimonidazole adducts were detected with a fluorescein isothiocyanate–conjugated specific antibody supplied with the kit (1:500). Stained sections were visualized with a confocal microscope (Fluoview FV10i, Olympus, Tokyo, Japan, www.olympus.co.jp) or a fluorescence microscope (Zeiss Axiovert 200M, Zeiss, Jena, Germany, www.zeiss.com).

Animal Procedures and Electroporation

All aspects of animal care and treatment were conducted according to the guidelines of the Experimental Animal Care Committee of Nara Institute of Science and Technology. The surgical procedures performed on pregnant ICR mice and embryo manipulations in utero were conducted as previously described [25]. E11.5 pregnant mice were deeply anesthetized by intraperitoneal injection with sodium pentobarbitone (50 μg/g b.wt.). HA–constitutively active HIF1α (HA-caHIF1α) cDNA was cloned into the EcoRI site of pCAGGS vector. After the uterus was exposed, approximately 1-2 μl of plasmid solution (1 μg/μl in phosphate-buffered saline) was injected into the lateral ventricle of the telencephalon with a glass micropipette. The embryos were held with the tips of a tweezers-type electrode with a diameter of 5 mm (CUY650-P3; Tokiwa Science, Fukuoka, Japan), and five electronic pulses (27V, 50 ms, at intervals of 950 ms) were given to each embryo with an electroporator (CUY21SC; Tokiwa Science). The embryos were reinserted into the abdominal cavity and the abdominal wall was closed with surgical sutures.

Exposure to High-Oxygen Atmosphere and Tissue Oxygen Measurement

The animal cage was placed in a hyperoxic oxygen chamber (Terucom, Kanagawa, Japan, www.terucom.co.jp). Oxygen tension was measured using a portable oxygen meter (Terucom) in the same chamber. E11.5 pregnant mice were exposed to 60% O_2 for 2 days, and the oxygen tension was then raised to 80% (the upper nonlethal concentration limit) and maintained at that level until fixation at E17.5.

Local tissue oxygen tension corresponding to each atmospheric oxygen level was measured with an OxyLab pO_2 monitor (Oxford Optronix, Oxford, UK, www.oxford-optronix.com) [26] (Supporting Information Fig. S4Q). The probe was

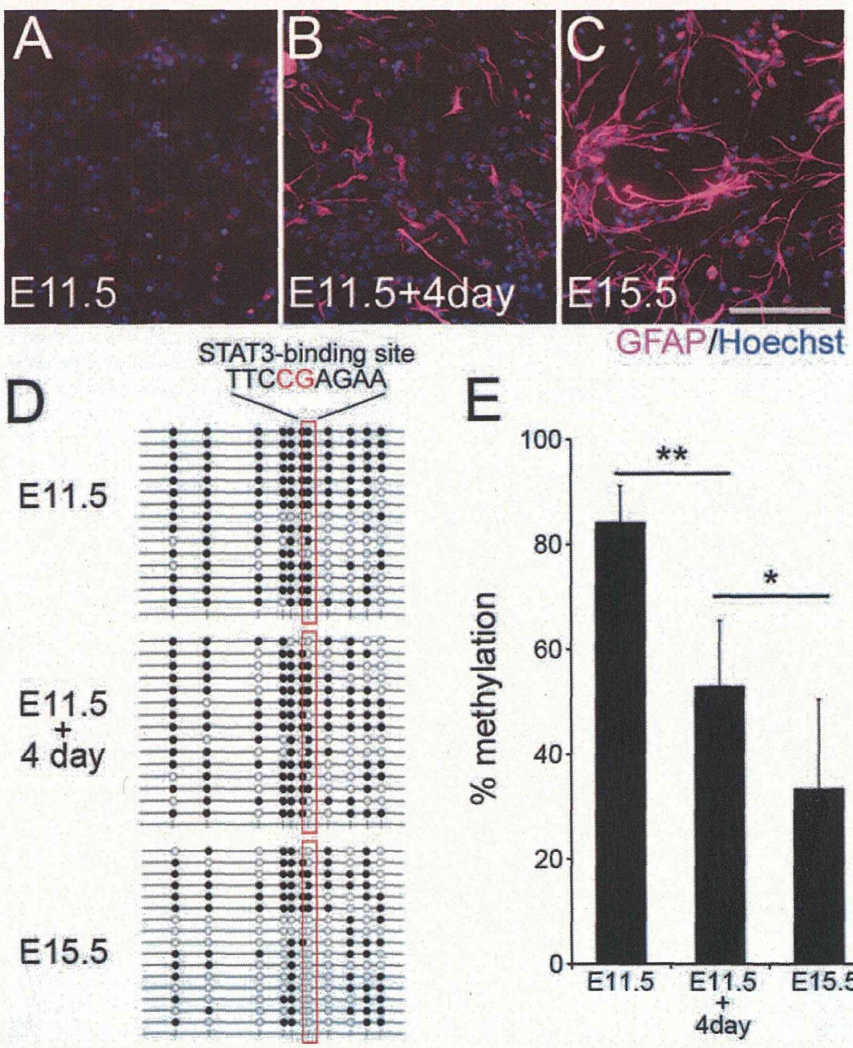

Figure 1. Astrocyte differentiation of midgestational neural precursor cells is retarded in vitro. **(A–C):** Leukemia inhibitory factor (LIF)-induced GFAP-positive astrocyte differentiation in E11.5 (A), in vitro 4-day-cultured E11.5 (B) and E15.5 (C) NPCs. After a 4-day culture in the presence of LIF, the cells were stained with anti-GFAP antibody (magenta) and with Hoechst to identify nuclei (blue). Scale bar = 100 μm. **(D, E):** Genomic DNA was extracted from the cells, and the methylation status of the *gfap* promoter around the STAT3-binding site was examined by bisulfite sequencing. Closed and open circles indicate methylated and unmethylated CpG sites, respectively (D). E11.5 and E15.5 indicate the results obtained for freshly prepared neural precursor cells (NPCs) from E11.5 cortex and E15.5 VZ. The STAT3-binding site is marked by red rectangles. Methylation at the STAT3-binding site in the *gfap* promoter is higher in 4-day in vitro-cultured E11.5 NPCs than in freshly prepared E15.5 NPCs (E). Data are shown as means ± SD ($n = 3$). Statistical significance was evaluated by the Student's t test. *, $p < .05$; **, $p < .01$. Abbreviations: GFAP, glial fibrillary acidic protein; STAT3, signal transducer and activator of transcription.

guided to the E15.5 brain using a 20-gauge needle with a plastic canula (Terumo, Tokyo, Japan, www.terumo.co.jp).

Results

It is well known that lgNPCs but not mgNPCs differentiate into astrocytes in response to stimulation with IL-6 family cytokines [2-5, 7]. When we cultured lgNPCs prepared from the VZ of mouse telencephalon at E15.5 (Supporting Information Fig. S1), we observed their LIF-induced astrocyte differentiation, as judged by the expression of the astrocytic marker GFAP (Fig. 1C, 26.8 ± 6.5%). By contrast, hardly any LIF-treated E11.5 mgNPCs differentiated into astrocytes (Fig. 1A). Interestingly, E11.5 mgNPCs cultured in vitro for 4 days (nominally corresponding to E15.5) did undergo astrocyte differentiation (Fig. 1B, 12.2 ± 1.9%), albeit to a lesser extent than E15.5 lgNPCs.

Since an inverse correlation exists between the potential of NPCs to express *gfap* and the methylation status of the *gfap* promoter, which includes a STAT3-binding site [5, 27], we examined whether the in vitro culture conditions of mgNPCs delayed the demethylation of the promoter compared to its demethylation in vivo. Bisulfite sequencing for the *gfap* promoter of E11.5, E11.5 + 4-day culture in vitro, and E15.5 NPCs revealed that this was indeed the case (Fig. 1D, 1E). These data indicate that the in vitro culture conditions retard the demethylation of the astrocytic gene promoter in NPCs.

In terms of the physical conditions surrounding cells, one of the biggest differences between in vitro and in vivo

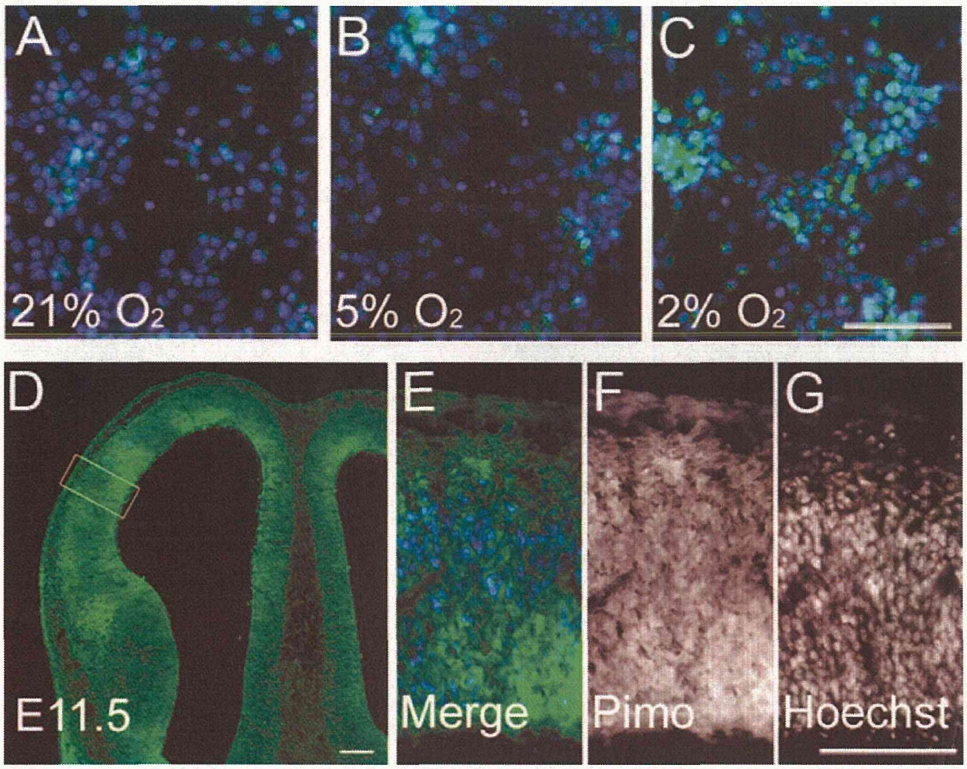

Figure 2. Oxygen levels are low in the embryonic brain. **(A–C):** Neural precursor cells cultured in 21% (A), 5% (B), or 2% O_2 (C) were stained with Hypoxyprobe. Pimonidazole adduct formation under hypoxic conditions (green) was observed clearly in 2% O_2 (C), less markedly in 5% O_2 (B), but not in 21% O_2 (A) (bar = 100 μm). **(D–G):** E11.5 embryonic brain was stained with Hypoxyprobe. Hypoxyprobe (green); Hoechst (blue). The image in (E) is an enlargement of the area in (D) marked by the rectangle. Bar = 100 μm.

environments is oxygen tension. The atmosphere contains 21% O_2 (160 mmHg), whereas interstitial oxygen concentration ranges from 1 to 5% (7-40 mmHg) in mammalian tissues including the embryonic brain [11, 20]. Although hypoxia is generally considered a pathological phenomenon, mammalian embryos develop naturally in a mildly hypoxic environment [28]. To determine the tissue oxygen tension in the embryonic brain, where NPCs reside, we used the chemical reagent pimonidazole. Pimonidazole is reductively activated in hypoxic cells and forms stable adducts with sulfhydryl groups in amino acids, at around or below 10 mmHg, which can be detected with specific antibodies [29, 30]. Pimonidazole adducts were weakly but clearly detected in NPCs cultured in 2% and 5% O_2 conditions, respectively, but not in NPCs cultured in 21% O_2 (Fig. 2A–2C). Pimonidazole adducts were also abundant in midgestational embryonic brain, indicating that oxygen levels there are low, particularly in the NPC-containing VZ (Fig. 2D–2G).

From the above findings, we hypothesized that culturing mgNPCs at a low oxygen level might accelerate their differentiation into astrocytes. To test this idea, mgNPCs were cultured in 2% or 21% O_2 atmospheres for 4 days in the presence of bFGF, and subsequently stimulated with LIF for an additional 4 days. As shown in Figure 3A–3C, a higher proportion of mgNPCs cultured in the presence of LIF under 2% O_2 than under 21% O_2 became GFAP-positive astrocytes. Reflecting the promotion of astrocyte differentiation, NPC (Nestin) and neuron (Map2ab) marker-positive cell numbers were lower under 2% O_2 than under 21% O_2 (Supporting Information Fig. S2A). The proliferation of cells in our normoxic and hypoxic culture was similar as judged by BrdU staining (Supporting Information Fig. S2B). Furthermore, in the 2% O_2 condition, significantly fewer CpG sites in the *gfap* promoter were methylated than in the 21% O_2 condition (Fig. 3D); this was also the case for CpG sites in the promoter of another astrocytic marker, *S100β* (Supporting Information Fig. S3A). Consistent with the lower methylation, *S100β* expression in hypoxic culture in the presence of LIF was higher than that in normoxic condition (Supporting Information Fig. S3B). These results suggest that low oxygen levels facilitate the DNA demethylation of astrocytic genes in mgNPCs.

We have shown previously that Notch signal activation induces the demethylation of astrocytic genes in mgNPCs [7]. Intriguingly, *hairy and enhancer of split 1* (*Hes1*) and *Hes5*, two known targets of Notch signaling, were markedly upregulated in the 2% O_2 culture condition (Fig. 4A), indicating that Notch signaling is more active at lower O_2 levels. Therefore, we examined whether low oxygen levels enhance the astrocyte differentiation of mgNPCs via Notch signal activation. An inhibitor of Notch signal activation, DAPT, was added to the culture medium during the first 4-day expansion phase of mgNPCs with bFGF in the hypoxic condition. The expression of *Hes1* and *Hes5* was dramatically reduced, confirming that hypoxia-induced elevation of Notch signaling was inhibited by DAPT (Supporting Information Fig. S3C). Furthermore, as shown in Figure 4B and 4C, the astrogenic potential of NPCs was almost completely suppressed by DAPT, and the enhanced demethylation of the *gfap* and *S100β* promoters observed in the hypoxic condition was no longer seen after DAPT treatment (Fig. 4D and Supporting Information Fig. S3D).

Activation of the Notch signaling pathway in mgNPCs induces expression of the transcription factor nuclear factor IA (NFIA), which leads to demethylation of astrocyte-specific genes including *gfap* [7]: NFIA binds to astrocytic gene

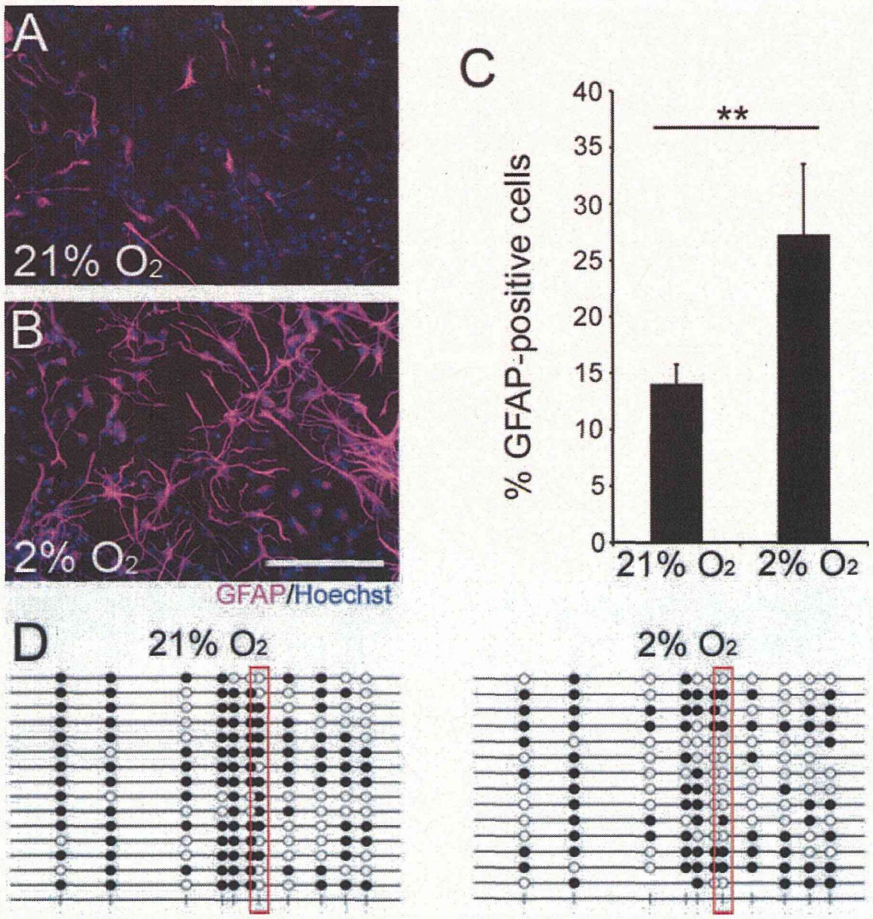

Figure 3. Culturing under 2% O_2 accelerates leukemia inhibitory factor (LIF)-induced astrocyte differentiation of neural precursor cells (NPCs). **(A–C):** E11.5 NPCs were cultured for 4 days under 2% O_2 (A) or 21% O_2 (B), followed by a 4-day LIF stimulation to induce astrocyte differentiation. GFAP (magenta), Hoechst (blue); bar = 100 μm. Proportions of GFAP-positive cells in the total cell populations were quantified (C). Data are shown as means ± SD ($n = 3$). Statistical significance was evaluated by the Student's t test. **, $p < .01$. **(D):** CpG methylation at the signal transducer and activator of transcription 3 (STAT3)-binding site in the *gfap* promoter is lower under 2% O_2 than under 21% O_2 after a 4-day culture of E11.5 NPCs. The STAT3-binding site is indicated by red rectangles. Abbreviation: GFAP, glial fibrillary acidic protein.

promoters and induces dissociation of DNA methyltransferase 1 (DNMT1) from the promoters, resulting in their demethylation. Therefore, we examined the expression of *Nfia* and found that it increased dramatically under the hypoxic condition (Supporting Information Fig. S4A). Moreover, we did not observe astrocyte differentiation of NFIA-deficient NPCs even when cultured with LIF under the hypoxic condition (Supporting Information Fig. S4B). Taken together, these findings suggest that activation of the Notch-NFIA cascade is the mechanism whereby hypoxia induces demethylation of the *gfap* promoter.

HIF1s have been shown to play important roles in cellular adaptation to hypoxia [11, 13, 31]. *HIF1α* and *HIF1β* are expressed in the developing mouse brain [32], and HIF1α protein accumulates to a higher level in hypoxic than in normoxic conditions as a result of increased transcription and protein stabilization [33–35]. Consistent with those observations, we found that both *HIF1α* transcript and nuclear HIF1α protein levels in E11.5 mgNPCs were upregulated under the 2% O_2 culture condition (Supporting Information Fig. S5A, S5B). Expression of the HIF1α target gene *Id1* was also upregulated (Supporting Information Fig. S5C), as was observed in neuroblastoma cells [12].

To determine whether HIF1α contributes to the hypoxia-promoted astrogenic potential of mgNPCs, we suppressed *HIF1α* mRNA using a specific shRNA. mgNPCs were prepared from E11.5 telencephalon and were infected the following day with lentiviruses expressing *HIF1α*-shRNA, cultured under 2% O_2 for 3 days, and then stimulated with LIF for a further 4 days. The level of *HIF1α* mRNA was reduced greatly in cells infected with *HIF1α* shRNA-expressing viruses (Supporting Information Fig. S6A). Moreover, *HIF1α* shRNA expression markedly diminished both the astrogenic potential of mgNPCs and the degree of demethylation in the *gfap* promoter (Fig. 5A–5G, and Supporting Information Fig. S6B).

caHIF1α is a hydroxylation-resistant, constitutively active mutant form of HIF1α in which two amino acids (prolines 402 and 564) are substituted with alanines [36]. One-day in vitro-cultured E11.5 mgNPCs were infected with lentiviruses expressing HA-tagged caHIF1α (HA-caHIF1α) and cultured for a further day, and then subjected to LIF stimulation for 3 days under the normoxic condition. HA-caHIF1α protein was clearly detected in the nucleus (Fig. 5M). In contrast to control virus-infected mgNPCs (Fig. 5H–5K), cells transduced to express HA-caHIF1α became GFAP-positive astrocytes in response to LIF stimulation, even under the 21% O_2 condition

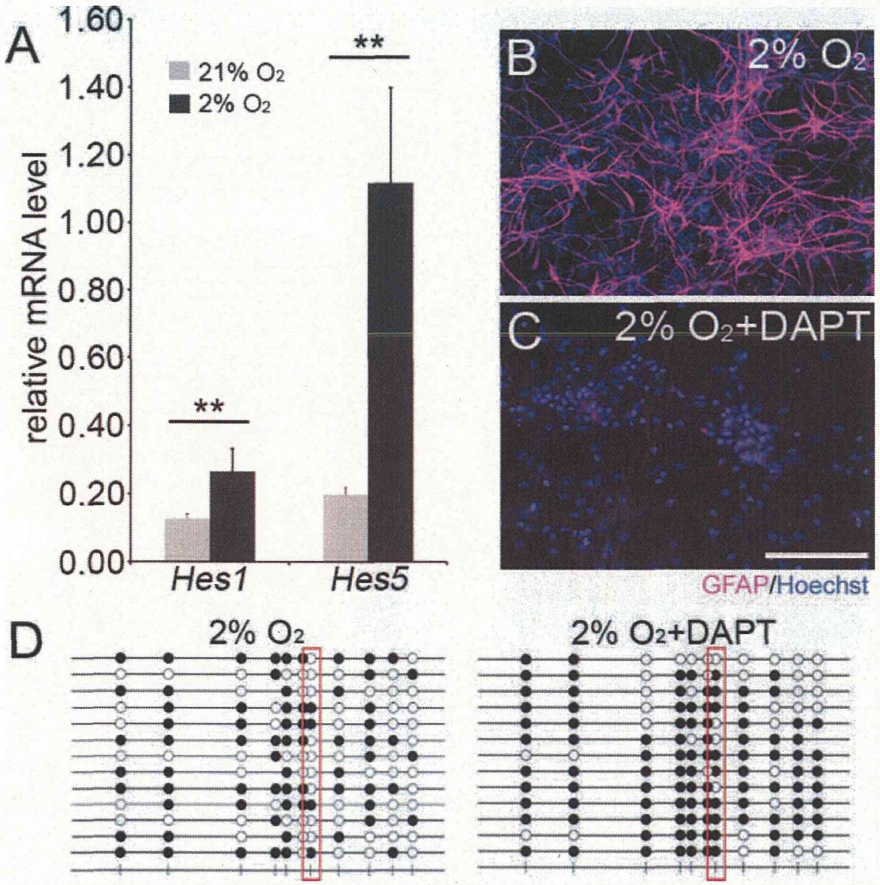

Figure 4. Notch signal activation is required for hypoxia-promoted acquisition of astrogenic potential by neural precursor cells (NPCs). **(A):** Quantitative polymerase chain reaction analysis of the expression of Notch signal target genes. Expression of the representative Notch signal targets *Hes1* and *Hes5* was upregulated in midgestational neural precursor cells cultured for 4 days under 2% O_2. Statistical significance was evaluated by the Student's *t* test. **, $p < .01$. **(B, C):** Hypoxia-induced astrogenic potential of NPCs was blocked by Notch signal inhibition. E11.5 NPCs were cultured for 4 days in the 2% O_2 condition with or without DAPT (10 μM), followed by a 4-day leukemia inhibitory factor stimulation. Bar = 100 μm. **(D):** The methylation status of the *gfap* promoter in E11.5 NPCs cultured with or without DAPT (10 μM) in the 2% O_2 condition was examined by bisulfite sequencing. The signal transducer and activator of transcription 3-binding site is indicated by red rectangles. Abbreviations: DAPT, *N*-[*N*-(3,5-difluorophenacetyl-L-alanyl)]-*S*-phenylglycine *t*-butyl ester); GFAP, glial fibrillary acidic protein.

(Fig. 5L–5O). HA-caHIF1α expression also augmented Notch signal activation in these cells (Fig. 5P). Furthermore, HA-caHIF1α-induced astrocyte differentiation and Notch signal activation were both abolished by DAPT treatment (Fig. 5P and Supporting Information Fig. S6C–S6J). Consistent with the results of these in vitro experiments, ectopic expression of HA-caHIF1α in E11.5 brains led to precocious GFAP expression in NPCs (Supporting Information Fig. S6K–S6P). These experiments suggest that HIF1α promotes the astrogenic potential of mgNPCs by enhancing Notch signal activation, probably because hypoxia-stabilized HIF1α can form a complex with the Notch intracellular domain (NICD) to effectively induce the expression of Notch-target genes [15].

Given that the 21% O_2 condition delayed the acquisition of astrocyte differentiation ability by NPCs in vitro, we next asked whether a hyperoxic environment has a similar effect on NPCs in vivo. To address this, pregnant mice were housed in a normoxic or hyperoxic chamber for 6 days (E11.5 to E17.5). To confirm that the embryonic brain was indeed under hyperoxia, we measured the local brain oxygen tension at E15.5 using an oxygen electrode. When the pregnant mice were in the normoxic (21% O_2) and hyperoxic (80% O_2) conditions, the oxygen tensions were 5.24 and 112.9 mmHg, respectively (Supporting Information Fig. S6Q), indicating that local brain oxygen tension was increased as a result of the atmospheric oxygen levels surrounding the pregnant mother mouse. After 6 days of hyperoxic housing, embryonic brains were then subjected to immunostaining and Western blotting. Interestingly, as shown in Figure 5Q–5S, exposure to high oxygen markedly decreased GFAP expression in the brains of embryos of mice housed in the hyperoxic condition.

These results suggest that a hypoxic environment is important for the proper timing of astrocyte differentiation during embryonic development.

Discussion

HIF1α is known to be an important factor in the response of various types of cells to hypoxic stress such as ischemia [11, 13] and to play a critical role in normal brain development [14]. In the present study, we have shown that astrocytic genes are progressively demethylated in the mildly hypoxic environment of the developing brain (Figs. 1–3). We further

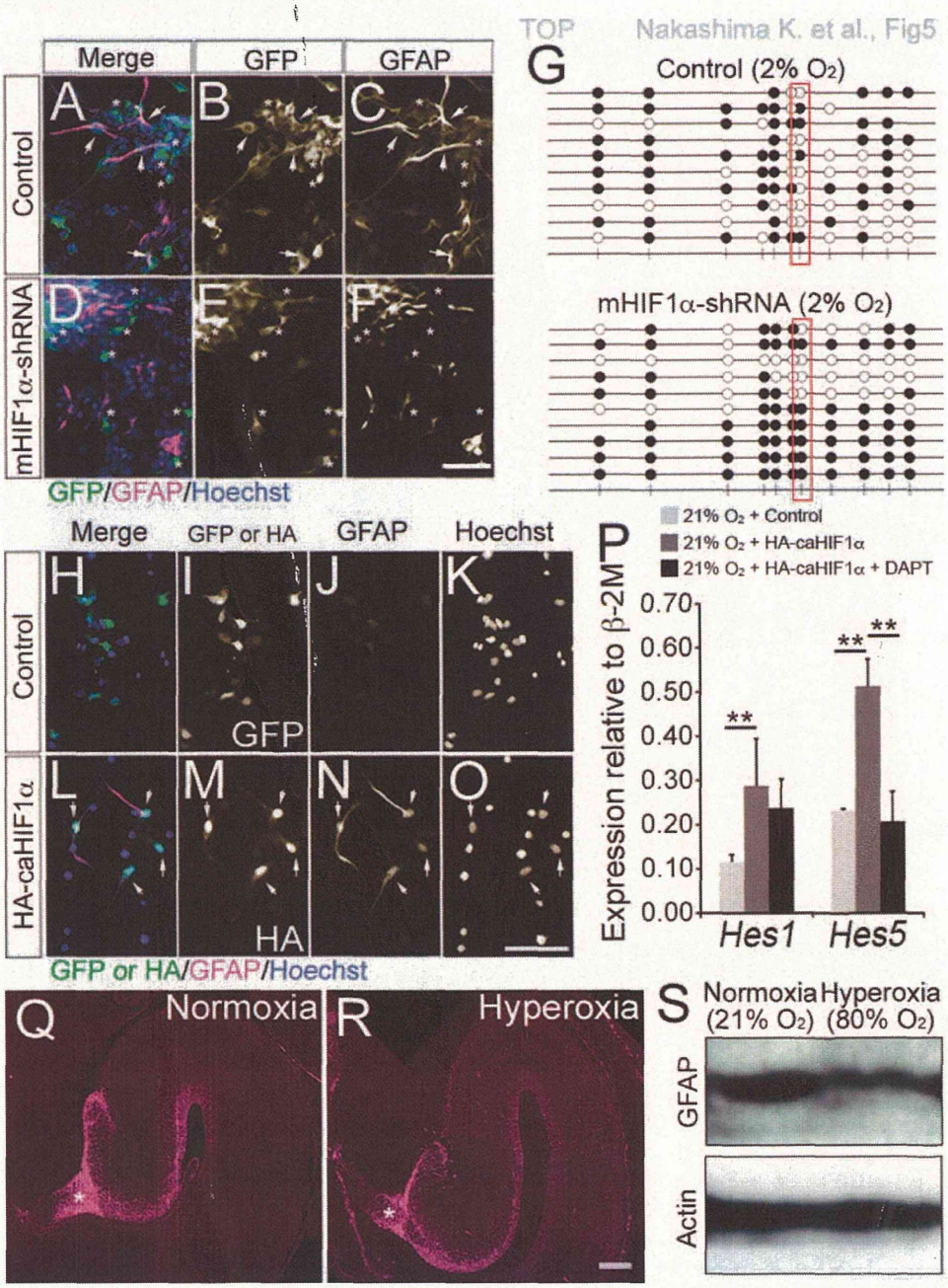

Figure 5. Astrogenic potential of neural precursor cells (NPCs) is regulated by HIF1α and oxygen levels. **(A–F):** E11.5 NPCs were infected with lentiviruses encoding GFP alone or GFP together with mHIF1α-shRNA, and cultured under 2% O_2 for 3 days followed by a 4-day leukemia inhibitory factor (LIF) stimulation. Virus-infected cells were identified by their GFP expression (green) and analyzed for GFAP expression (magenta) by immunocytochemistry. Hoechst, blue. GFP and GFAP double-positive cells (arrows) were observed in control virus-infected cells (A–C), whereas most of the mHIF1α-shRNA-expressing virus-infected cells were positive for GFP only (asterisks) (D–F). Bar = 50 μm. **(G):** The methylation status of the *gfap* promoter in 3-day-cultured virus-infected cells was examined by bisulfite sequencing. Demethylation in mHIF1α-shRNA-expressing virus-infected cells was inhibited. The signal transducer and activator of transcription 3-binding site is indicated by red rectangles. **(H–O):** Hydroxylation-mediated degradation-resistant constitutively active HIF1α (HA-caHIF1α) was introduced into E11.5 NPC by lentivirus infection, and the cells were cultured for 1 day followed by a 3-day LIF stimulation under 21% O_2. Precocious GFAP expression was observed in HA-caHIF1α-expressing virus-infected cells (arrows), even under 21% O_2 (L–O). Bar = 50 μm. **(P):** E11.5 NPCs were infected with control or HA-caHIF1α-expressing lentiviruses on the day after preparation and cultured in the presence of LIF for 3 days with or without DAPT under 21% O_2, and their RNAs were then subjected to quantitative polymerase chain reaction. *Hes1* and *Hes5* expression was normalized to that of β-2M. The expression of both of these genes was upregulated by HA-caHIF1α expression, and this effect was abolished by DAPT treatment. Statistical significance was evaluated by the Student's *t* test. **, $p < .01$. **(Q, R):** GFAP expression in E17.5 brain was reduced when pregnant mice were housed in a hyperoxic atmosphere (80% O_2) from E11.5 to E17.5. Brain sections are stained with anti-GFAP antibody (magenta). Hippocampal regions are shown as representatives. Asterisks, fimbria. Bar = 100 μm. **(S):** Whole brains of embryos from pregnant mice housed in normoxic (21% O_2) and hyperoxic (80% O_2) atmospheres were lysed and subjected to immunoblot to detect GFAP and β-actin (as loading control) expression. Abbreviations: β-2M, β-2 microglobulin; caHIF1α, constitutively active HIF1α; DAPT, *N*-[*N*-(3,5-difluorophenacetyl-L-alanyl)]-*S*-phenylglycine *t*-butyl ester); GFAP, glial fibrillary acidic protein; GFP, green fluorescent protein; HA, hemagglutinating; mHIF1α, mouse HIF1α; shRNA, short hairpin RNA.